 doi:10.20944/preprints201608.0044.v1

Article

Multiple Layers of Silicon-Silica (Si-SiO_2) Pair onto Silicon Substrate towards Highly Efficient, Wideband Silicon Photonic Grating Coupler

Md Asaduzzaman [1,2,*], Masuduzzaman Bakaul [1,3], Stan Skafidas [1] and Md Rezwanul Haque Khandokar [1,2]

[1] Department of Electrical and Electronic Engineering, The University of Melbourne, Parkville, VIC 3010, Australia
[2] CSIRO (Commonwealth Scientific and Industrial Research Organisation), 343 Royal Parade, Parkville, VIC 3052, Australia
[3] School of Engineering, Monash University Malaysia, 47500 Bandar Sunway, Selangor, Malaysia
* Correspondence: m.asaduzzaman@student.unimelb.edu.au

Abstract: A single mode waveguide grating coupler based on multiple Si-SiO_2 pairs onto Si substrate has been designed. Numerical analysis has been carried out to calculate optimum thickness of the layers of Si-SiO_2 that ensures the constructive interference between reflected waves and actual guided wave for high coupling efficiency. Based on the results, an optimal design is developed and modeled by using a 2-D finite difference time domain (2-D FDTD) simulator that dictates a coupling efficiency of as much as 78% (-1.07 dB) at the wavelength of 1550 nm, and a 1-dB bandwidth of 77 nm. The numerical method will be useful to calculate the optimum thicknesses of the layers for any reflector based grating coupler of different materials.

Keywords: grating coupler; silicon photonics; optical interconnects; fiber interface; nanophotonics

1. Introduction

In recent years, nanoscale photonic technologies have attracted a lot of attention to co-develop photonic and electronic devices on silicon (Si) to provide a highly integrated electronic–photonic platform [1]. Silicon-on-insulator (SOI) technology that relies heavily on the contrasted indices of Si and SiO_2, enables the design and integration of these photonic devices in submicronic scales, similar to the devices produced by a standard CMOS fabrication platform in electronic industry [2, 3]. One of the key challenges with these submicronic waveguide devices is enabling efficient coupling with fiber, which is caused mainly due to the mode-field differences between fiber and the waveguide, and the relative misalignments [4]. To overcome this challenge, various techniques including prism, butt, and grating coupling have been proposed. Among them, although butt coupling is an elegant solution for low loss and wideband operation, it often requires post processing for accurate polishing and dicing to taper the waveguide edges. Therefore, it is not suitable for wafer-scale testing [5-8]. Grating couplers, which mostly perform out of the plane coupling between a fiber and a waveguide, are also an attractive solution as light can be coupled in and out everywhere on the chip, opening the way for wafer-scale testing [9, 10].

However, despite such advantages, grating coupler often exhibits low coupling efficiency (CE) due to downward radiation of light that propagates towards substrate through buried oxide (BOX) which comprises 35%-45% of total incident light [11]. To minimize this propagation, various attempts have been made by improving the directionality such as poly-silicon gate layer based [12] and poly-silicon overlay based [13] grating coupler with CE of 74% and 78% respectively both of which require an additional layer of amorphous Si layer. A fully etched photonic crystal based uniform gating coupler is demonstrated with CE of 42% [14]. CE of 65% is reported in [15] by optimizing the grating parameters. An apodized grating coupler with theoretical CE of 72% is

Preprints (www.preprints.org) | NOT PEER-REVIEWED | Posted: 4 August 2016 doi:10.20944/preprints201608.0044.v1

reported in [16] by through-etched gratings. A subwavelength grating coupler by implementing waveguide dispersion engineered subwavelength structures is designed in [17] with CE of -2.72 dB. A comprehensive design method is presented in [18] for achieving high CE in grating coupler where demonstrated CE of -0.62 dB is reported with nonuniform grating and using metal back mirror. An engineered RI of materials using fully etched photonic crystal holes in apodized grating is presented in [19] with demonstrated CE of 67%. By suppressing the second order Brag reflection from the grating using asymmetric grating structure, the CE of 80% is reported in [20] with nonuniform grating for perfectly vertical coupling. A binary blazed grating coupler for perfectly vertical and near vertical coupling is proposed in [21] with CE of 75% and 84% respectively. The above solutions have offered high directionality for improving CE, however, most designs are based on apodized and nonuniform grating which often require complex steps in CMOS process in compare to uniform grating.

Apart from optimization of grating structures and parameters, insertion of mirror in the BOX is another solution to avoid the downward radiation in grating coupler. A grating coupler based on gold bottom mirror is proposed in [22] with theoretical and demonstrated CE of 72% and 69% respectively. However addition of gold mirror requires many extensive steps which are not compatible with CMOS. Another back side metal (aluminum) based grating coupler is demonstrated in [23] to enhance directionality with CE of 69%. Although this design avoids wafer-to-wafer bonding technique for adding aluminum layer, it is still beyond the scope of Si photonics as materials being used other than Si. Based on Distributed Brag Reflector (DBR) a design is proposed in [24] with theoretical CE of 92% where the grating are nonuniform. In [25] the downward radiating light has been reflected toward waveguide using a stack of amorphous-Si/ SiO_2 Bragg bottom reflectors with theoretical and demonstrated CE of 82% and 69.5% respectively where the dimensions of Si and SiO_2 layers needs to be exactly of quarter wavelength.

In this paper we propose an all-Si uniform grating coupler based on a new wafer structure with multiple pairs of poly Si-SiO_2 onto Si-substrate. The thicknesses of the layers are analyzed numerically and derived mathematical equations to calculate optimum thicknesses for constructive interference to enhance CE of the reflector based grating coupler. This paper has taken a top-down approach to examine the issues related to a reflector based grating coupler for high CE. The characteristic parameters of the structure was studied, analyzed and optimized to achieve highly efficient and wideband grating coupler. Based on the optimized parameters, a design was developed and modeled by using a finite difference time domain (FDTD) simulator. The performance of the designed coupler was also thoroughly characterized for better clarity.

2. Proposed Wafer Structure with Multiple Pairs of Si-SiO_2 onto Si-Substrate

As indicated earlier, coupling efficiency largely relies on how successfully the part of light passing through the BOX and the Si-substrate of a typical single layered structure can be reflected towards the waveguide. To enable such reflection, instead of a thicker SiO_2 BOX layer, a wafer structure with multiple thinner layers of Si-SiO_2 pair onto Si-substrate can be developed, a schematic diagram of which is shown in figure 1. Shown in figure 1, each Si-SiO_2 interface acts as a mirror to reflect certain amount of light, and after several reflections, most of the light passed through the BOX and the Si-substrate combines with the light towards the waveguide. The insertion of Si and SiO_2 layers however isn't straightforward, as the structure will complement coupling efficiency only if the reflected light waves from the Si-SiO_2 interfaces interfere constructively with the originally guided light wave towards the waveguide. Therefore, to enable constructive interference, the path lengths traveled by the reflected light and the angle of interference at Si-SiO_2 interfaces have to be chosen carefully.

Shown in figure 1, let us assume that the reflected lights from the interfaces of Si and SiO_2 layers of a m-pair structure reach the top Si waveguide with angles $\theta_{r1}, \theta_{d11}, \theta_{d12}, \theta_{d13}, \theta_{d14}$ and θ_{d1n}.

These angles mainly depend on the angle of incidence θ_{in} and the refractive indices (RIs) of Si and

Preprints (www.preprints.org) | NOT PEER-REVIEWED | Posted: 4 August 2016 doi:10.20944/preprints201608.0044.v1

SiO_2, which by using the basic laws of refraction, can be shown to be equal to each other and calculated as,

$$\theta_{d1} = \sin^{-1}\left[\left(\frac{n_{top}}{n_{si}}\right)\sin\theta_{in}\right] \quad (1)$$

where n_{top} and n_{si} are the RIs of top cladding (air) and Si waveguide respectively. θ_{in} is the angle of incidence measured clockwise from the normal to the gratings.

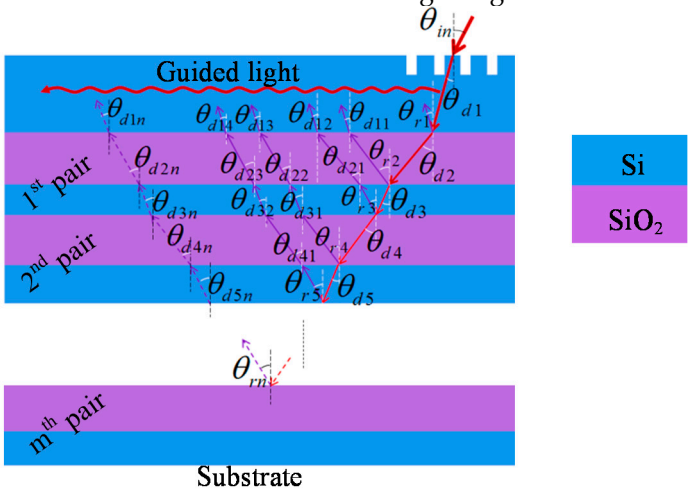

Figure 1. Proposed structure with multiple layers of Si and SiO_2 (BOX) pair onto Si-substrate that reflects the light passing through the BOX and the Si-substrate of a typical single layered BOX structure to interfere with the actual guided light wave at the waveguide. Only primary reflections towards waveguide are shown.

The pattern of interference that is expected to happen due to the superposition of the reflected light with the actual guided light can be determined by the difference of path lengths (PL) travelled by each wave of interest. Shown in figure 1, there are two primary reflections per pair. Using Eq. (1) and geometry of the structure, the PL for each reflected wave and the corresponding guided wave can be calculated as follows:

Path lengths travelled by the waves for the 1st pair of Si-SiO_2 can be calculated by

$$\left.\begin{aligned}
PL_{ref_{11}} &= 2\frac{t_{SiO_2}}{\cos\left[\sin^{-1}\left[\frac{n_{top}}{n_{SiO_2}}\sin\theta_{in}\right]\right]} \\
PL_{wave_{11}} &= 2\sqrt{\left[\frac{t_{SiO_2}}{\cos\left[\sin^{-1}\left[\frac{n_{top}}{n_{SiO_2}}\sin\theta_{in}\right]\right]}\right]^2 - t_{SiO_2}^2} \\
PL_{ref_{12}} &= 2\left[\frac{t_{si}}{\cos\left[\sin^{-1}\left[\frac{n_{top}}{n_{si}}\sin\theta_{in}\right]\right]} + \frac{t_{SiO_2}}{\cos\left[\sin^{-1}\left[\frac{n_{top}}{n_{SiO_2}}\sin\theta_{in}\right]\right]}\right] \\
PL_{wave_{12}} &= 2\left[\sqrt{\left[\frac{t_{si}}{\cos\left[\sin^{-1}\left[\frac{n_{top}}{n_{si}}\sin\theta_{in}\right]\right]}\right]^2 - t_{si}^2} + \sqrt{\left[\frac{t_{SiO_2}}{\cos\left[\sin^{-1}\left[\frac{n_{top}}{n_{SiO_2}}\sin\theta_{in}\right]\right]}\right]^2 - t_{SiO_2}^2}\right]
\end{aligned}\right\} \quad (2)$$

where $PL_{ref_{11}}$ and $PL_{ref_{12}}$ are the PLs for the reflected waves for SiO_2 and Si layers of 1st pair respectively, $PL_{wave_{11}}$ and $PL_{wave_{12}}$ are corresponding PLs for the guided waves, t_{SiO_2} and t_{Si} are the thicknesses of the SiO_2 layer and Si layer of the pair, n_{top}, n_{SiO_2} and n_{Si} respectively are the RIs

Preprints (www.preprints.org) | NOT PEER-REVIEWED | Posted: 4 August 2016 doi:10.20944/preprints201608.0044.v1

for the top cladding, SiO_2 and Si layers, and θ_{in} is the angle of incidence of light at the surface of the waveguide.

To enable constructive interference between reflected and actual guided light, the difference of PLs needs to be an integer multiple of wavelength which can be calculated as

$$\begin{aligned} \Delta PL_{11} &= PL_{ref_{11}} - PL_{wave_{11}} = \left(k - \tfrac{1}{2}\right)\lambda \\ \Delta PL_{12} &= PL_{ref_{12}} - PL_{wave_{12}} = k\lambda \end{aligned} \tag{3}$$

where ΔPL is the path length difference between reflected and actual guided light, k is an integer and λ is the wavelength of the light.

Using Eq. (2) and (3), the value of k can be calculated for the thicknesses of SiO_2 and Si at which k is an integer as shown in figure 2 (a). Figure 2 (b) shows the incident angles at which the k is an integer.

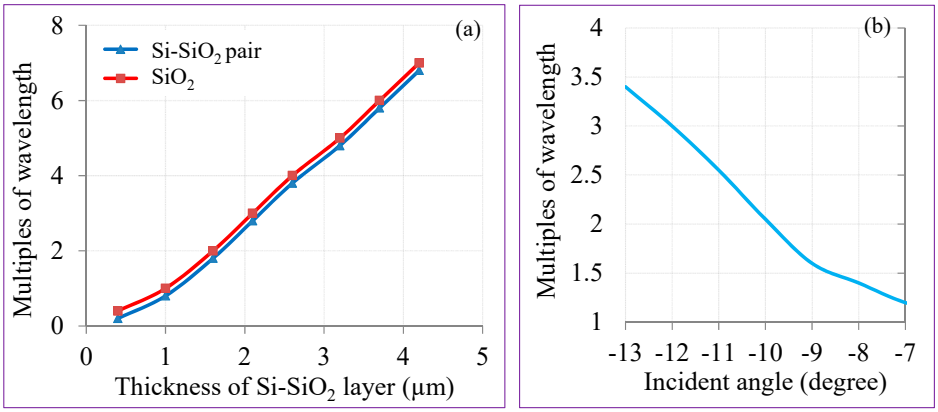

Figure 2. Multiples of wavelengths for (a) thicknesses of the SiO_2 and Si (b) incident angle

Shown in figure 2, the integer values of k occur at the thicknesses of 1.000 µm ($k=1$), 1.600 µm ($k=2$), 2.100 µm ($k=3$), 2.600 µm ($k=4$), 3.200 µm ($k=5$), 3.700 µm ($k=6$), 4.200 µm ($k=7$) of SiO2. Using Eq. (3), the thickness of SiO_2 (t_{SiO_2}), Si (t_{Si}) and thickness of Si-SiO_2 pair (t_{pair}) at which the constructive interferences occur are shown in table 1.

Table 1: Thicknesses of the 1st pair for constructive interference between reflected and guided light.

Value of k	1	2	3	4	5	6	7
t_{SiO_2} (µm)	0.500	1.100	1.600	2.100	2.600	3.200	3.700
t_{Si} (µm)	0.100	0.100	0.100	0.100	0.100	0.100	0.100
t_{pair} (µm)	0.600	1.200	1.700	2.200	2.700	3.300	3.800

The PLs for subsequent pairs can be expressed in terms of PLs of the 1st pair as

$$\begin{aligned} PL_{ref_{mn}} &= \begin{cases} \dfrac{m+n}{2} PL_{ref_{11}} + \dfrac{m-n}{2} PL_{ref_{12}}, n=1 \\ \dfrac{m+1}{n} PL_{ref_{12}} + \dfrac{m}{n} PL_{ref_{11}}, n=2 \end{cases} \\ PL_{wave_{mn}} &= \begin{cases} mPL_{wave_{11}} + (m-n) PL_{wave_{12}}, n=1 \\ m\left(PL_{wave_{11}} + PL_{wave_{12}}\right), n=2 \end{cases} \end{aligned} \tag{4}$$

Preprints (www.preprints.org) | NOT PEER-REVIEWED | Posted: 4 August 2016 doi:10.20944/preprints201608.0044.v1

where m is the number of pair and n is the layer of SiO_2 $(n=1)$ and Si $(n=2)$ of the m^{th} pair.

Using Eq. (3) and (4) the optimum thickness of 2nd pair can be calculated at which the value of k is an integer for constructive interference between reflected and guided light. Shown in figure 3, the integer values of k happen at the thicknesses of SiO_2 of 400 nm, 900 nm, 1400 nm and 1900 nm. Therefore the total thicknesses of the 2nd pair can be obtained by adding 100 nm of Si with the thicknesses of SiO_2.

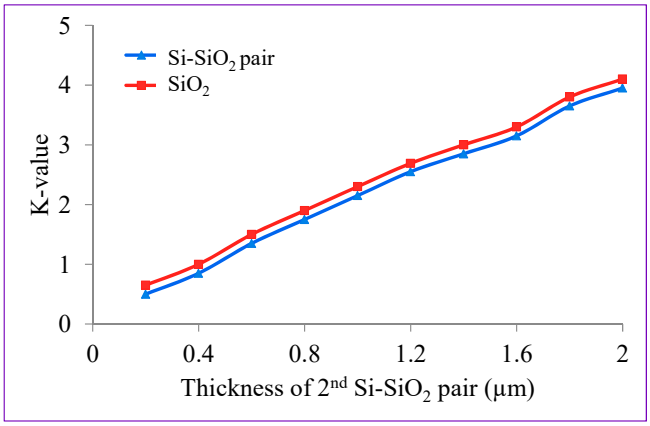

Figure 3. Values of k for the different thicknesses of 2nd pair of $Si\text{-}SiO_2$

3. Designed Grating Coupler based on the Proposed Multi-layer Structure

The schematic diagram and the specifications of the grating coupler designed based on the proposed multi-layer structure is shown in figure 4. It consists of a SOI wafer with top Si layer of 220 nm for single mode operation of the coupler. The BOX layer is incorporated with two pairs of $Si\text{-}SiO_2$, with top pair of 500 nm SiO_2 and 100 nm Si layers and bottom pair of 400 nm SiO_2 and 100 nm Si. The gratings are etched at the top Si layer. The grating period (Λ) is calculated using the equation below [26]:

$$\Lambda = \frac{\lambda}{n_{eff} - n_{top}\sin(\theta_{in})} \tag{5}$$

where λ is the wavelength of light incident on the surface of the grating structure, n_{eff} is the effective RI of the structure, n_{top} is the RI of the top cladding, and θ_{in} is the angle of incidence with normal to the surface of the structure. By using fully vectorial mode solver of LumericalTM [27], n_{eff} is found to be 2.006, and by setting target wavelength at $\lambda = 1550$ nm, $n_{top} = 1$ (air), and $\theta_{in} = -12^0$, grating period is calculated to be 700 nm. The etch depth (d) and grating width (w) are also optimized for maximum efficiency and found to be 80 nm and 400 nm respectively, with a filling factor (w/Λ) of 0.571. Therefore, after etching the grating depth of 80 nm, a 140 nm silicon layer remains as waveguide below the gratings.

Preprints (www.preprints.org) | NOT PEER-REVIEWED | Posted: 4 August 2016 doi:10.20944/preprints201608.0044.v1

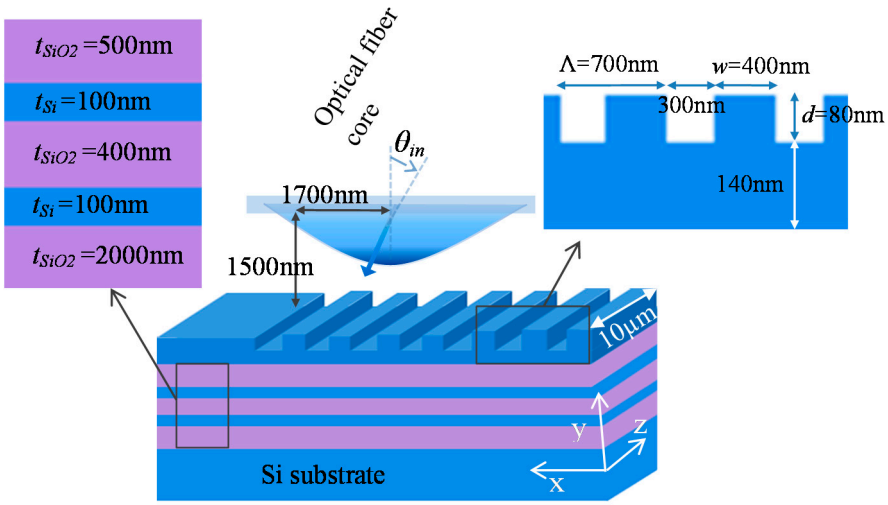

Figure 4. Schematic diagram of the proposed multi-layer structure grating coupler with design parameters.

The fabrication of the proposed structure is fully compatible with standard CMOS process technology. To develop a photonic circuitry, a 2 μm SiO_2 layer for isolation can be deposited on a bare silicon wafer using high density plasma. To deposit the reflector layers on SiO2, the surface of SiO_2 layer is needed to be polished by chemical mechanical polish (CMP). After deposition of reflector layers comprising of 100 nm Si 400 nm SiO_2 100 nm Si 500 nm SiO_2 by high density plasma, a 220 nm layer of poly-Si can be deposited by plasma enhanced chemical vapour deposition (PECVD) process. Finally, the grating structure can be realized on top Si layer using 193 nm optical lithography and dry etching.

4. Performance Characterization and Discussion

The proposed grating coupler is simulated using 2-D FDTD of Lumerical Solutions™, a commercially available software package to design silicon photonics devices [28]. A TE polarized Gaussian shaped light source is applied on the surface of the gratings with Mode-Field Diameter of 10 μm which is comparable with standard single mode fiber (SMF). The position of the optical source is optimized as 1500 nm above the grating surface and 1700 nm away from the left end of grating as shown in figure 4. The TE mode field distribution in the BOX and the silicon waveguide region including the impinging Gaussian beam region is shown in figure 5. Figure 5(a) shows the propagation of light when there was only BOX layer (SiO_2) on the Si substrate and figure 5(b) shows the propagation at the presence of multiple layers of Si-SiO_2 pairs onto Si-substrate.

For fair comparison, other parameters of the coupler were kept unchanged. Shown in figure 5(b), light through the BOX layer has been reduced significantly at the presence of Si-SiO_2 layers. Figures 5(c)-(d) show the TE mode profiles of light from the point of incidence of the grating coupler along the Si waveguide. The incident light, that is scattered by the surface gratings, propagates in +x, –x, and –y directions. The lights along +x and -x directions diffract upwards and interfere with the incident light which form a standing wave with resonance around the point of incidence. As a result, maximum light occurs at the point of incident (x = -5.5 μm) which is 1700 nm away from the left-most end of the grating, as shown in figures 5(c)-(d). The addition of Si-SiO_2 layers onto Si-substrate increases the light up to 78% (figure 5 (d)) whereas light was about 40% without Si-SiO_2 layers (figure 5 (c)). This is due to the fact that light propagating through the BOX and Si-substrate was never collected back and wasted completely. The Si-SiO_2 layers onto Si-substrate reflect the wasted light back to the waveguide and recollected to increase the delivery of optical power.

Preprints (www.preprints.org) | NOT PEER-REVIEWED | Posted: 4 August 2016 doi:10.20944/preprints201608.0044.v1

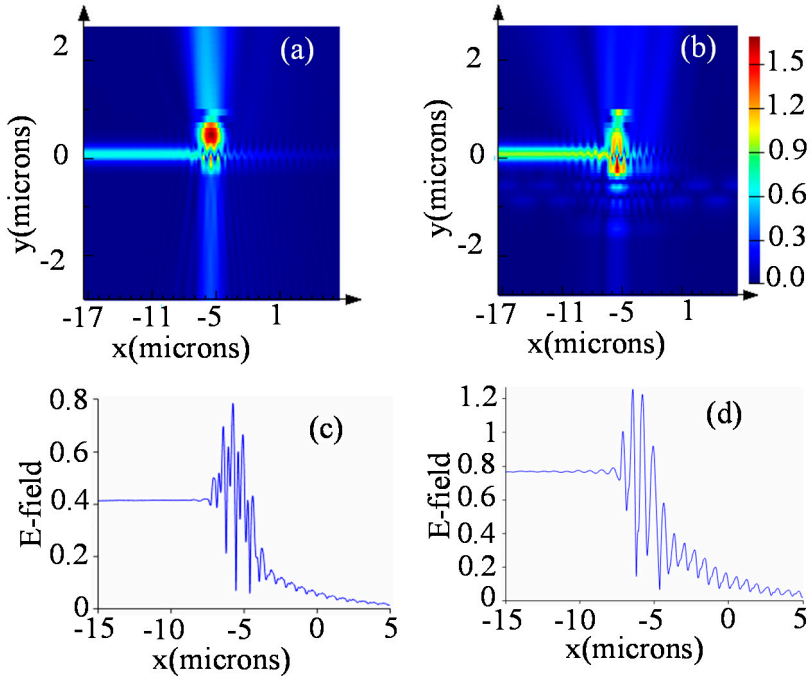

Figure 5. TE mode distribution of light in the proposed grating coupler at the wavelength of 1550 nm for the structures (a): without any Si-SiO_2 pair inside the BOX, and (b): with Si-SiO_2 layers inside the BOX. (c) and (d) represent the respective profiles of the TE mode of light for the structures again without and with Si-SiO_2 layers inside the BOX.

To achieve high CE, the thickness of the SiO_2 at which constructive interference happen has been chosen based on equations (2) and (3). Figure 6 shows the CE over a range of telecommunications wavelengths where it can be seen that the maximum CE is achieved for the BOX thicknesses at which the value of k in Eq. (3) is an integer. Figure 6(a) shows CE for SiO_2 thicknesses of constructive interference whereas figure 6(b) shows CE for some SiO_2 thicknesses of destructive interference where the value of k is other than an integer. Shown in figure 6(a), the maximum CE happens at the thicknesses of 500 nm, 1100 nm, 1600 nm, 2100 nm as obtained in table1 using Eq. (2) and (3). Although high CEs (81% and 80%) are achieved at the thickness of 1100 nm at 1557 nm wavelength and at the thickness of 1600 nm at 1554 nm wavelength respectively, the CEs are over narrow wavelength range. For the thickness of 500 nm, the high CE (78%) is achieved over wide range of wavelengths. When the thicknesses of SiO_2 such that the value of k is apart from an integer, the CE decreases as shown in figure 6(b). As the difference between thicknesses at which k is an integer and non-integer increases, the CE keep decreasing.

Similarly, the thickness of the 2nd pair can be calculated using Eq. (3) and (4) at which the value of k is an integer and hence the waves interfere constructively. Figures 6 (c) and (d) show the CE over a range of wavelengths for the thicknesses of 2nd pair. For the thicknesses of 400 nm, 900 nm, 1400 nm and 1900 nm of SiO_2 of 2nd pair where the k vale is an integer and the waves interfere constructively and the CE enhanced to around 78% over a wide range of wavelength as shown in figure 6(c) where as for the thicknesses of SiO_2 at which the k value is other than an integer, the waves interfere destructively and the CE falls lower as shown in figure 6(d).

Preprints (www.preprints.org) | NOT PEER-REVIEWED | Posted: 4 August 2016 doi:10.20944/preprints201608.0044.v1

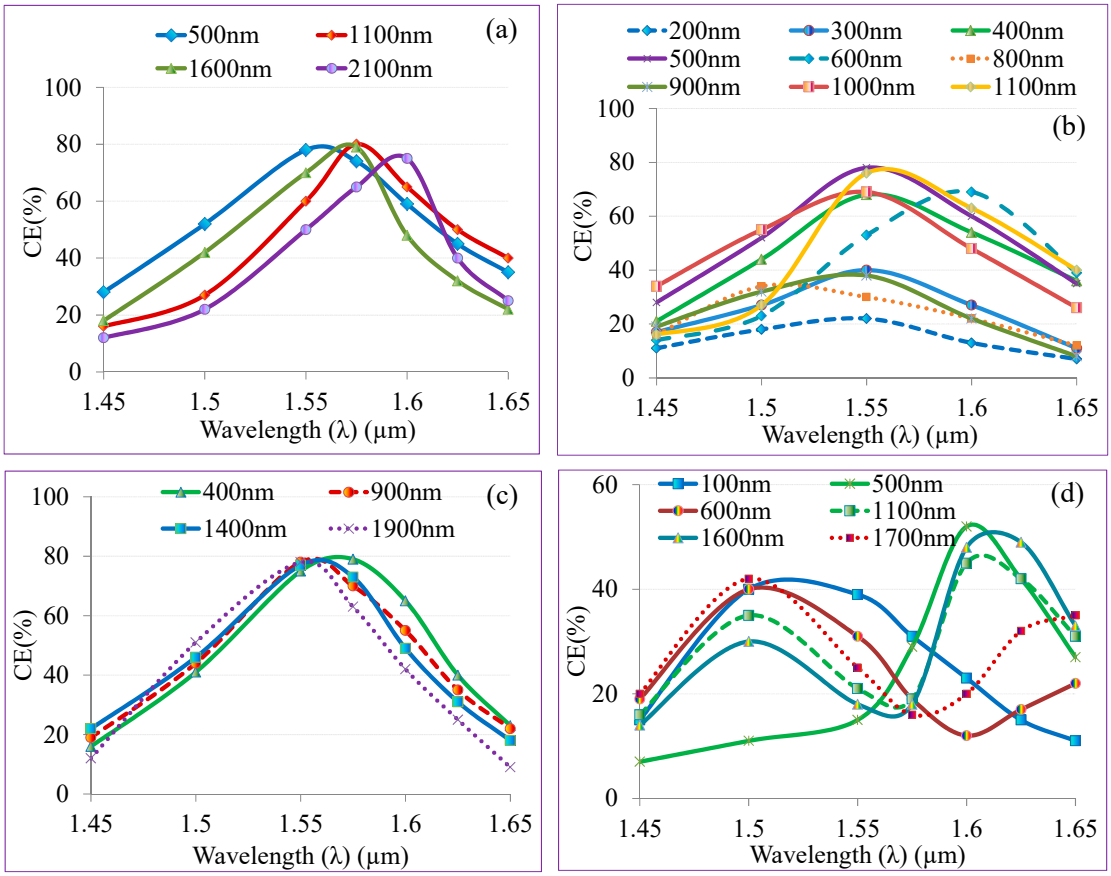

Fig.6. Coupling efficiency vs wavelengths (a) thicknesses of SiO_2 for which k is an integer and hence constructive interference occurs (b) thicknesses of SiO_2 from 200 nm to 1100 nm. At 500 nm and 1100 nm thicknesses constructive interferences occur and deviation from these thicknesses results in destructive interference which causes lower CE (c) for different thicknesses of 2nd pair of Si-SiO_2 where constructive interferences occur (d) for different thicknesses of 2nd pair of Si-SiO_2 where destructive interferences occur.

To quantify the optimum values of CE and CBW, the proposed coupler is characterized for various performance influencing parameters including (i) position of the fiber (optical source) on the grating surface, (ii) angle of incidence, (iii) grating filling factor, (iv) etch depth and waveguide thickness (v) number of Si-SiO_2 pairs onto Si-substrate. From here on all the characterization of influencing parameters is performed by keeping the mirror thickness and position constant.

The relationships among various axial positions (both horizontal and vertical) of fiber on the grating surface, coupling efficiency and coupling bandwidth are shown in Fig. 7 (a). It shows that the horizontal positioning of fiber has a significant effect on both CE and CBW, whereas, vertical positioning has very little to do in this regard. The maximum coupling efficiency (CE = 78%, -1.07 dB) and bandwidth ($CBW_{1\text{-}dB}$ = 77 nm) are achieved at 1500 nm above the grating surface and 1700 nm away from the left-most starting point of the grating structure. Fig. 7 (b) characterizes various CEs and CBWs with different angles of incidence of light. It shows that CE follows approx. periodic highs and lows with the changes in angles of incidence and the picture is quite different for CBWs, which shows a gradual decrease from the highest value due to the changes in angles of incidence. The figure also shows that the highest CE and CBW both happen at an incident angle of around -12^0.

Preprints (www.preprints.org) | NOT PEER-REVIEWED | Posted: 4 August 2016 doi:10.20944/preprints201608.0044.v1

Coupling bandwidth of any grating coupler is highly reliant on the grating filling factor (ff), where higher ff enables more light to couple to the waveguide of longer wavelengths, and lower ff enables to couple more light of shorter wavelengths. The CEs in regard to wavelengths for 80% ff and 30% ff are shown in Fig. 8 (b). In order to achieve higher coupling bandwidths, the ff must be chosen in such a way that the coupling of light for both longer and shorter wavelengths is optimized simultaneously. In our design the optimized filling factor ($ff = w/\Lambda$) is 57.1% at which the maximum bandwidth is achieved. The thickness of the Si waveguide is optimized as 220 nm and grating is formed by etching this layer. The optimum etch depth is found to be 80 nm which is 40% of the waveguide thickness for maximum coupling efficiency and bandwidth as shown in Fig. 8 (a).

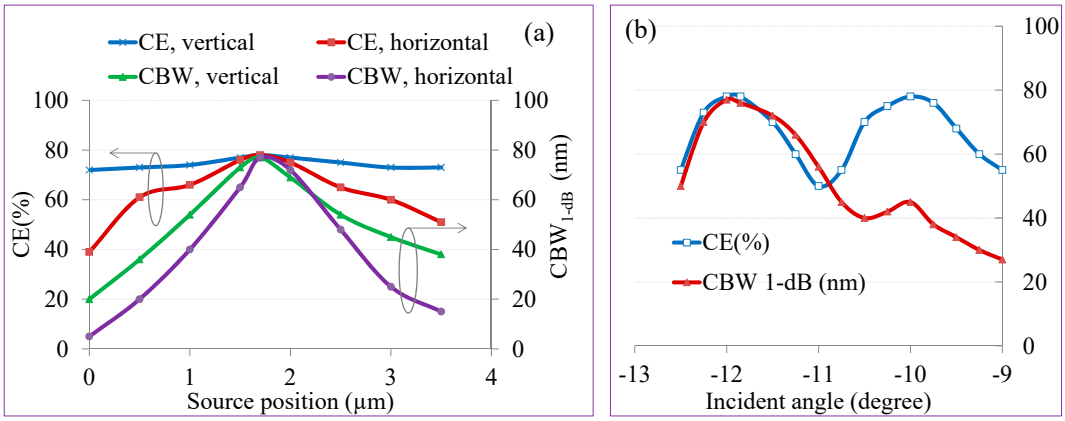

Fig. 7. (a): The relationships among various axial (both vertical and horizontal axis) positions of the fiber on the grating surface, coupling efficiency at wavelength of 1550 nm and coupling bandwidth. "0" in the horizontal scale refers the left-most starting point of the grating structure (b): The relationships among various incident angles, coupling efficiency at wavelength of1550 nm and coupling bandwidth.

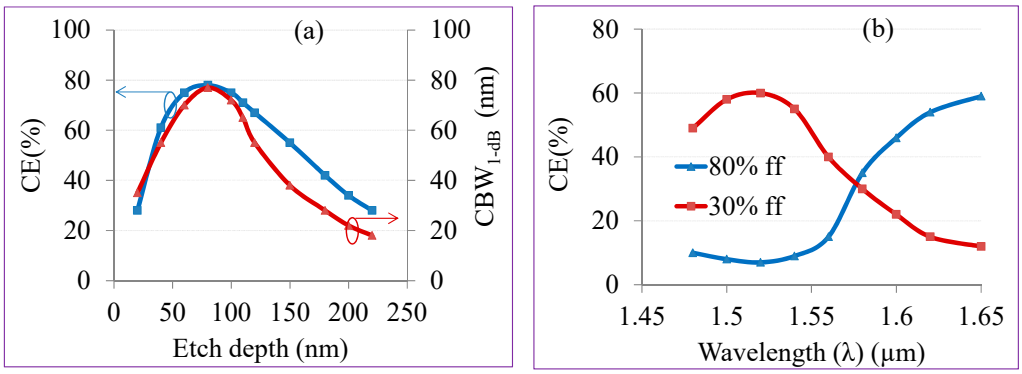

Fig. 8. (a): Coupling efficiency at wavelength of 1550 nm and bandwidth with respect to the etch depth. "0" in horizontal scale refers non-etched and "220" as fully-etched for the waveguide thickness of 220 nm (b): Coupling efficiency vs. wavelength for higher and lower grating filling factors.

Preprints (www.preprints.org) | NOT PEER-REVIEWED | Posted: 4 August 2016 doi:10.20944/preprints201608.0044.v1

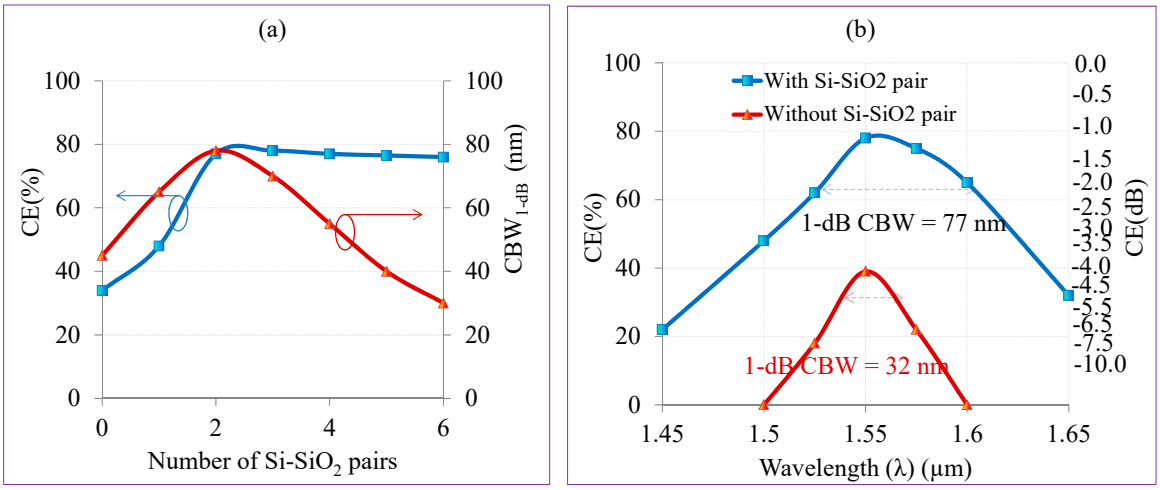

Fig. 9. (a): Coupling efficiency at wavelength of 1550 nm and bandwidth for number of Si-SiO2 pair inside the BOX (b): coupling bandwidth of the proposed grating coupler, with and without reflective pairs.

Fig. 9 (a) characterizes the coupling efficiency at the wavelength of 1550 nm and bandwidth for number of Si-SiO2 pairs in the BOX layer. It shows that coupling efficiency keeps increasing until virtually saturated after just two Si-SiO2 pairs whereas coupling bandwidth decreases with number of additional Si-SiO2 pairs after two as shown in Fig. 9 (a).

With such optimized values of fiber positions (1500 nm above the grating surface and 1700 nm from left-most end of the gratings), incident angle ($\theta_{in} = -12^0$), grating period ($\Lambda = 700\,nm$), filling factor ($ff = 57.1\%$), etch depth (80 nm), waveguide thickness ($t_{wg} = 220\,nm$) and two pairs of Si-SiO2 on Si substrate, the 1-dB coupling bandwidth of the proposed coupler is recalculated and found to be 77 nm as shown in Fig. 9 (b).

5. Conclusion

We have numerically analyzed the downward radiation in reflector based grating coupler. Results show that the thicknesses of the BOX and reflector layers are the decisive factors for designing highly efficient grating coupler. We developed mathematical formulas specifically for reflector based grating coupler that can readily be used to calculate the optimum thicknesses of the layers for high coupling efficiency. Based on the findings, a highly efficient and wideband grating coupler with multiple Si-SiO2 pair in the BOX layer has been designed with achieved coupling efficiency of 78% (-1.07 dB) at the wavelength of 1550 nm, and 1-dB bandwidth of 77 nm. In our knowledge, this is the highest designed coupling efficiency and bandwidth reported together for any diffraction based grating coupler. The coupling efficiency can further be improved over 90% by minimizing the back reflection and implementing the mode matching condition between optical fiber and waveguide modes which can be achieved using apodized grating.

References

1. G.T. Reed, The optical age of silicon. *Nature* **2004**, 427, 595–596.

2. Haishan Sun, Antao Chen, Attila Szep, and Larry R. Dalton, Efficient fiber coupler for vertical silicon slot waveguides, *Opt. Express* **2009**, 17(25), 22571-22577.
3. Xiaochuan Xu, Harish Subbaraman, John Covey, David Kwong, and A. Hosseini, Complementary metal-oxide-semiconductor compatible high efficiency subwavelength grating couplers for silicon integrated photonics, *Appl. Phys. Lett.* **2012**, 101, 0311091.
4. G. Roelkens, D. Vermeulen, D. Van Thourhout, S. B. R. Baets, P. G. P. Lyan, and J.-M. Fédéli, High efficiency diffractive grating couplers for interfacing a single mode optical fiber with a nanophotonic silicon-on-insulator waveguide circuit, *Appl. Phys. Lett.* **2008**, 92, 131110.
5. Graham T. Reed and Andrew P. Knights, *Silicon Photonics an Introduction*, John Wiley & Sons Ltd, UK, 2004.
6. T. Shoji, T. Tsuchizawa, T. Watanabe, K. Yamada, and H. Morita, Low loss mode size converter from 0.3 μm square Si wire waveguides to single mode fibres, *Electron. Lett.* **2002**, 38, 1669-1670.
7. V. R. Almeida, R. R. Panepucci, and M. Lipson, Nanotaper for compact mode conversion, *Opt. Lett.* **2003**, 28, 1302-1304.
8. S. McNab, N. Moll, and Y. Vlasov, Ultra-low loss photonic integrated circuit with membrane-type photonic crystal waveguides, *Opt. Express* **2003**, 11, 2927-2939.
9. Neil Na, Harel Frish, I-Wei Hsieh, Oshrit Harel, Roshan George, Assia Barkai, and Haisheng Rong, Efficient broadband silicon-on-insulator grating coupler with low backreflection, *Opt. Lett.* **2011**, 36, 2101-2103.
10. Tapas Kumar Saha and Weidong Zhou, High efficiency diffractive grating coupler based on transferred silicon nanomembrane overlay on photonicwaveguide, *J. Phys. D: Appl. Phys.* **2009**, 42, 085115, 1-9.
11. D. Vermeulen, S. Selvaraja, P. verheyen, G. Lepage, W. Bogaerts, P. Absil, D. Van Thourhout, G. Roelkens, High-efficiency fiber-to-chip grating couplers realized using an advanced CMOS-compatible Silicon-On-Insulator platform, *Opt. Express* **2010**, 18, 18278-18283.
12. Chao Qiu, Zhen Sheng, Le Li, Albert Pang, Zhiqi Wang, Aimin Wu, Xi Wang, Shichang Zou, and Fuwan Gan, Poly-Silicon Grating Couplers for Efficient Coupling With Optical Fibers, *IEEE Photon. Technol. Lett.* **2012**, 24, 1614-1617.
13. G. Roelkens, D. Van Thourhout, and R. Baets, High efficiency Silicon-on-Insulator grating coupler based on a poly-Silicon overlay, *Opt. Express* **2006**, 14, 11622-30.
14. Liu Liu, Minhao Pu, Kresten Yvind, and Jørn M. Hvam, High-efficiency, large bandwidth silicon-on-insulator grating coupler based on a fully-etched photonic crystal structure, *Appl. Phys. Lett.* **2010**, 96, 0511261-3.
15. Zhe Xiao, Feng Luan, Tsung-Yang Liow, Jing Zhang, and Ping Shum, Design for broadband high-efficiency grating couplers, *Opt. Lett.* **2012**, 37, 530-532.
16. Mikael Antelius, Kristinn B. Gylfason, Hans Sohlstrom, An apodized SOI waveguide-to-fiber surface grating coupler for single lithography silicon photonics, *Opt. Express* **2011**, 19, 3592-3598.
17. Qiuhang Zhong, Venkat Veerasubramanian, Yun Wang, Wei Shi, David Patel, Samir Ghosh, Alireza Samani, Lukas Chrostowski, Richard Bojko, David V. Plant, Focusing-curved subwavelength grating couplers for ultra-broadband silicon photonics optical interfaces, *Opt. Express* **2014**, 22, 18224-18231.
18. Wissem Sfar Zaoui, Andreas Kunze, Wolfgang Vogel, Manfred Berroth, Jörg Butschke, Florian Letzkus, Joachim Burghartz, Bridging the gap between optical fibers and silicon photonic integrated circuits, *Opt. Express* **2014**, 22, 1277-1286.
19. Yunhong Ding, Haiyan Ou, Christophe Peucheret, Ultrahigh-efficiency apodized grating coupler using fully etched photonic crystals, *Opt. Lett.* 2013, 38, 2732-2734.
20. Günther Roelkens, Dries Van Thourhout, Roel Baets, High efficiency grating coupler between silicon-on-insulator waveguides and perfectly vertical optical fibers, *Opt. Lett.* 2007, 32, 1495-1497.
21. Li Yu,LuLiu, ZhipingZhou, XingjunWang, High efficiency binary blazed grating coupler for perfectly-vertical and near-vertical coupling in chip level optical interconnections, *Optics Communications* **2015**, 355, 161-166.
22. F. Van Laere, G. Roelkens, J. Schrauwen, D. Taillaert, P. Dumon, W. Bogaerts, D. Van Thourhout, R. B aets, Compact grating couplers between optical fibers and Silicon-on-Insulator photonic wire waveguides with 69% coupling efficiency, in Proceedings of IEEE Conference on Optical Fiber Communication, (OFC 2006), pp. 1-3.
23. Wissem Sfar Zaoui, María Félix Rosa, Wolfgang Vogel, Manfred Berroth, Jörg Butschke, Florian Letzkus, Cost-effective CMOS-compatible grating couplers with backside metal mirror and 69% coupling efficiency, *Opt. Express* **2012**, 20, 238-243.

24. D. Taillaert, P. Bienstman, R. Baets, Compact efficient broadband grating coupler for silicon-on-insulator waveguide, *Opt. Lett.* **2004**, 29, 2749-51.
25. Shankar Kumar Selvaraja, Diedrik Vermeulen, Marc Schaekers, Erik Sleeckx, Wim Bogaerts, Gunthe Roelkens, Pieter Dumon, Dries Van Thourhout, Roel Baets, Highly efficient grating coupler between optical fiber and silicon photonic circuit, in Conference on Lasers and Electro-Optics, Technical Digest (CD) (Optical Society of America, 2009), paper CTuC6.
26. J. V. Galan, P. Sanchis, J. Blasco, J. Marti, Study of High Efficiency Grating Couplers for Silicon-Based Horizontal Slot Waveguides, *IEEE Photon. Technol. Lett.* **2008**, 20, 985-987.
27. Lumerical Solutions inc. http://www.lumerical.com/tcad-products/mode (accessed on 05/07/2016).
28. Lumerical Solutions inc. http://www.lumerical.com/tcad-products/fdtd (accessed on 05/07/2016).